

Quantum decay of the persistent current in a Josephson junction ring

D. A. Garanin and E. M. Chudnovsky

*Physics Department, Lehman College, The City University of New York,
250 Bedford Park Boulevard West, Bronx, NY 10468-1589, U.S.A.*

(Dated: November 16, 2015)

We study the persistent current in a ring consisting of $N \gg 1$ Josephson junctions threaded by the magnetic flux. When the dynamics of the ring is dominated by the capacitances of the superconducting islands the system is equivalent to the xy spin system in 1+1 dimensions at the effective temperature $T^* = \sqrt{2JU}$, with J being the Josephson energy of the junction and U being the charging energy of the superconducting island. The numerical problem is challenging due to the absence of thermodynamic limit and slow dynamics of the Kosterlitz-Thouless transition. It is investigated on lattices containing up to one million sites. At $T^* \ll J$ the quantum phase slips are frozen. The low- T^* dependence of the persistent current computed numerically agrees quantitatively with the analytical formula provided by the spin-wave approximation. The high- T^* behavior depends strongly on the magnetic flux and on the number of superconducting islands N . Depending on the flux, the persistent current gets destroyed by the phase slips and/or by the superconductor-insulator transition on increasing T^* .

PACS numbers: 74.50.+r, 74.81.Fa, 73.23.Ra, 75.30.Kz

I. INTRODUCTION

Microscopic chains of Josephson junctions have been at the forefront of research on quantum phase transitions^{1,2} and quantum circuitry³⁻⁵. They provide a testing field for two fundamental physical effects: Quantum phase slips⁶⁻⁸ and superconductor-insulator transition⁹⁻¹². Persistent currents in small metallic rings have been studied theoretically and experimentally since 1960s¹³ while the studies of microscopic Josephson junction rings are more contemporary. They are rapidly advancing due to the progress in manufacturing of the nanostructures¹².

Analytical research on Josephson junction rings focused on two limits: When the dynamics of the ring is dominated by the capacitances of the junctions¹⁴ and when the dynamics is dominated by the capacitances of the superconducting islands¹⁵. Also the mixed situation with both capacitances has been studied. The persistent currents were computed numerically for the rings containing up to 40 superconducting islands¹⁶, as well as analytically using the effective low-energy description⁸. Quantum phase slips in a Josephson junction chain have been studied experimentally¹⁷ and the good agreement with theoretical concepts¹⁵ has been demonstrated.

Our interest to the problem has been motivated by the strong size effect observed in the previous numerical studies of the persistent currents in relatively small Josephson junction rings, Fig. 1. It demonstrated the necessity to study longer chains with a large number of superconducting islands N . The case when the dynamics of the ring is dominated by the capacitances of the islands, that is considered here, permits such large- N analysis because the quantum 1d problem of the ring maps onto a classical $2d$ xy spin model at a finite temperature that is well suited for large-scale Monte Carlo (MC) studies.

The equilibrium persistent current in a Josephson junc-

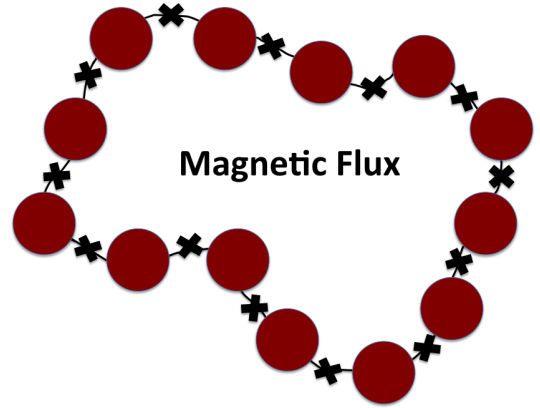


Figure 1: Color online: A ring of N Josephson junctions (crosses) made of superconducting grains (circles), threaded by the magnetic flux.

tion ring threaded by the magnetic flux depends on the value of the flux. It may be destroyed by temperature or by quantum fluctuations. The measure of the strength of quantum fluctuations is the ratio of the charging energy of the superconducting island, U , and the Josephson coupling between the islands, J . Exact mapping of the problem onto the $2d$ xy spin problem allows one to express the effect of quantum fluctuations at zero temperature in terms of the effective “quantum” temperature $T^* = \sqrt{2JU}$. The Kosterlitz-Thouless (KT) temperature, $T_{KT} \sim J$, at which the quasi-long-range order in the $2d$ model is destroyed by the unbinding of vortex-antivortex pairs provides the critical value of U that results in the superconductor-insulator transition.

When the flux is different from $(n + 1/2)\Phi_0$, where n is an integer and Φ_0 is the flux quantum, the equilibrium persistent current has a non-zero value as long

as quantum fluctuations are weak $T^* < T_{KT}$. With increasing quantum fluctuations one should expect the persistent current to become zero at $T^* = T_{KT}$. The situation is more complicated in the half-fluxon case, $\Phi = (n + 1/2)\Phi_0$, when quantum phase slips provided by vortices of the $2d$ xy classical model connect, via quantum tunneling, the states with persistent currents running in opposite directions. In this case the MC routine elucidates the fact that while the persistent current is theoretically metastable at any non-zero U , the phase slips are frozen at $T^* \ll T_{KT}$, making small Josephson junction rings to resemble superparamagnetic particles.

The numerical solution of the problem is challenging in comparison with the typical problems of magnetic phase transitions for two reasons. First, the persistent current is a mesoscopic quantity that becomes small for a large system size, $I \propto 1/N$. This is why the increase in the system size does not lead to a significant improvement of the results via self-averaging. At high quantum temperatures the root-mean-square fluctuations of the persistent current, $\sqrt{\langle I^2 \rangle} \propto 1/N$, decrease with the size but so does the current itself. The second reason is that the $2d$ xy model does not exhibit a dramatic change in the spin-spin correlation function due to the unbinding of vortex-antivortex pairs. The (pseudo)dynamics of this process is extremely slow. It requires a large number of updates and computer runs.

The paper is structured as follows. The theory is given in Section II. The model of a Josephson junction ring whose dynamics is dominated by capacitances of superconducting islands is formulated in Section II A. The equivalence of the model to the xy spin model in 1+1 dimensions at finite temperature is reviewed in Section II B. Persistent current and its T^* -dependence expected from the theory are discussed in Section II C. Numerical results are presented in Section III. The numerical method is described in Section III A. Formation of vortices responsible for the phase slips and for quantum KT transition is discussed in Section III B. In Section III C we present numerical results on the destruction of the persistent current by quantum fluctuations. The energy barrier for the phase sleep is analyzed in Section IV. Section V contains some final remarks and suggestions for experiment.

II. THEORY

A. Ring made of Josephson junctions

Consider a Josephson junction ring depicted in Fig. (1). Let θ_j be the phase of the superconducting order parameter $\Psi = |\Psi| \exp(i\theta)$ at the j -th superconducting island. The Josephson energy of the ring is then given

by¹⁸

$$E_J = J \sum_i \left[1 - \cos \left(\theta_{i+1} - \theta_i + \frac{2\pi}{\Phi_0} \int_i^{i+1} \mathbf{A} \cdot d\mathbf{l} \right) \right], \quad (1)$$

where the vector potential \mathbf{A} is due to the magnetic flux Φ piercing the ring.

The summation of phases along the closed loop of the ring gives

$$\sum_i \left(\theta_{i+1} - \theta_i + \frac{2\pi}{\Phi_0} \int_i^{i+1} \mathbf{A} \cdot d\mathbf{l} \right) = 2\pi(\phi + m), \quad (2)$$

where $\phi \equiv \Phi/\Phi_0$, $\Phi_0 = h/(2e)$ is the flux quantum, and m is an arbitrary integer. This can be derived by computing the flux through the ring as $\Phi = \oint \mathbf{A} \cdot d\mathbf{l}$ and noticing that the superconducting current $\mathbf{j}_s = \frac{e\hbar}{m} |\Psi|^2 \left(\nabla\theta - \frac{2\pi}{\Phi_0} \mathbf{A} \right)$ is zero inside the islands since we only have Josephson currents in the system.

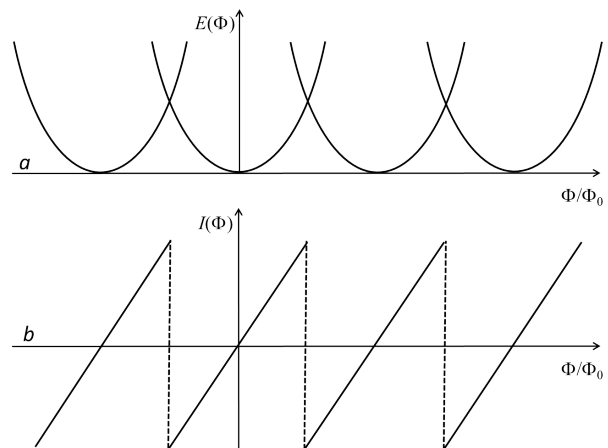


Figure 2: (a) m -branches of the ground-state energy $E_J^{(0)}$. (b) m -branches of the persistent current.

Eq. (2) allows one to write

$$E_J = J \sum_i \left[1 - \cos \left(\tilde{\theta}_{i+1} - \tilde{\theta}_i + \frac{2\pi(\phi + m)}{N} \right) \right], \quad (3)$$

where the reduced phases $\tilde{\theta}$ are defined in such a way that the change of $\tilde{\theta}_i$ around the ring is zero. The total change in the original phase θ accumulated around the ring is accounted for by the quantum number m . These reduced phases are convenient for the analytical work, whereas the numerical work uses the original phases. The energy minimum corresponds to all phases being the same, leading to the ground state

$$E_J^{(0)} = NJ \left[1 - \cos \left(\frac{2\pi(\phi + m)}{N} \right) \right] \cong \frac{(2\pi)^2 J}{2N} (\phi + m)^2, \quad (4)$$

the last expression being the large- N case. Branches of $E_J^{(0)}(\Phi)$ for different values of m are shown in Fig. 2a.

When $\phi = n + 1/2$, with n being an integer, that is for $\Phi = (n + 1/2)\Phi_0$, the ground state is degenerate, $E_J(n, m) = E_J(n, m') = -2n - m - 1$. This permits quantum tunneling between $E_J(n, m)$ and $E_J(n, m')$ that removes the degeneracy. For, e.g., $n = 0$, that is, when the flux equals half a fluxon, $\Phi = \Phi_0/2$ ($\phi = 1/2$), the states with $m = 0$ and $m = -1$, corresponding to different current states in the ring, have the same energy. Quantum oscillations between such states have been observed in experiment^{21,22}.

B. Dynamics

The dynamics of the model is due the electrical charging of the superconducting islands by the excess (or lack) of Cooper pairs n_i at the i -th site. It is determined by the finite capacitances of the islands and of the junctions. In this paper we are considering the limit in which the capacitances of the islands C greatly exceed the capacitances of the junctions. This situation can be easily achieved in experiment. For example it will occur when the Josephson junctions are formed by the weak links between small superconducting grains. In this case the charging energy is given by

$$E_C = \sum_i U n_i^2 = \frac{\hbar^2}{4U} \sum_i \left(\frac{d\theta_i}{dt} \right)^2 \quad (5)$$

where $U = (2e)^2/(2C)$. The second of Eq. (5), which plays the role of the kinetic energy, is obtained by noticing that n_i and θ_i are canonically conjugated variables. If they are treated quantum-mechanically, one has

$$n_i = -i \frac{d}{d\theta_i}, \quad i\hbar \frac{d\theta_i}{dt} = [\theta_i, E_C] = 2iU n_i \quad (6)$$

Quantum mechanics of the model is formulated in terms of the path integral

$$I = \prod_i \int D\{\theta_i(\tau)\} e^{-S_E/\hbar} \quad (7)$$

where $\tau = it$ and $S_E = \int d\tau \mathcal{L}$ is the Euclidean action with

$$\begin{aligned} \mathcal{L} = & \frac{\hbar^2}{4U} \sum_i \left(\frac{d\theta_i}{d\tau} \right)^2 \\ & + J \sum_i \left[1 - \cos \left(\theta_{i+1} - \theta_i + \frac{2\pi\phi}{N} \right) \right]. \end{aligned} \quad (8)$$

Here the phases θ_i are the original phases, as in Eq. (1), not the reduced phases of Eq. (3).

This quantum model at $T = 0$ is equivalent¹ to the statistical mechanics of the classical model in $1+1$ dimensions at a non-zero temperature $T^* = \sqrt{2JU}$, described by the partition function

$$Z = \prod_i \int D\{\theta_i(\tau)\} e^{-\mathcal{H}_{1+1}/T^*} \quad (9)$$

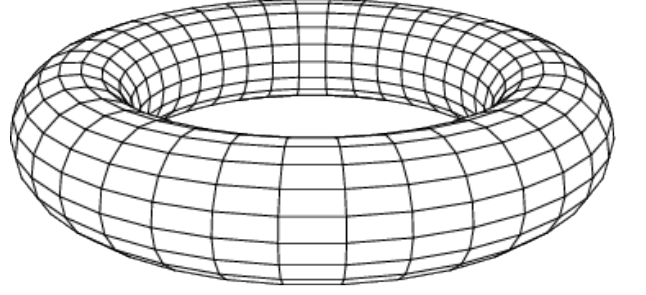


Figure 3: $(1+1)d$ space-time lattice with periodic boundary conditions used in numerical work.

with

$$\mathcal{H}_{1+1} = -\frac{1}{2} \sum_{\mathbf{r}\mathbf{r}'} J_{\mathbf{r}\mathbf{r}'} \cos(\theta_{\mathbf{r}'} - \theta_{\mathbf{r}} + \phi_{\mathbf{r}\mathbf{r}'}), \quad (10)$$

where \mathbf{r} is a discrete two-dimensional vector $\mathbf{r} = (i, l)$ representing the space-time lattice, while $J_{\mathbf{r}\mathbf{r}'} = J$ for the nearest neighbors and zero otherwise. In the numerical work we use the $N \times N$ lattice with periodic boundary conditions that correspond to the surface of a toroid, Fig. 3. The circumference of the cross-section of the toroid along the closed i direction contains N sites corresponding to N superconducting islands in the Josephson junction ring. The l direction along the length of the toroid corresponds to the imaginary time. Phase shifts are given by $\phi_{i,l;i\pm 1,l} = \pm 2\pi\phi/N$ and $\phi_{i,l;i,l\pm 1} = 0$. Notice that, in principle, the periodic boundary condition imposed on the imaginary time (our closed x direction) introduces a finite physical temperature into the original quantum problem, $T \sim T^*/N$. At large N the effect of that temperature on the persistent current can be ignored.

The statistical model presented above can be reformulated in terms of the two-component classical spin vectors of the $2d$ xy model at temperature $T^* = \sqrt{2JU}$ that describes the strength of quantum fluctuations. As is known, the $2d$ xy model exhibits the Kosterlitz-Thouless phase transition at^{19,20} $T_c \approx 0.89J$. For the quantum model this means that on increasing the charging energy U quantum fluctuations become sufficiently strong to destroy Josephson currents. It is believed that the corresponding quantum phase transition results in the state of the ring (sometimes called the Cooper-pair insulator) in which the islands connected by Josephson junctions maintain their superconductivity but no Josephson current can circulate in the ring. The natural way to test this interpretation of the quantum KT phase transition is to study the U -dependence of the persistent Josephson current in the ring.

C. Persistent current

In accordance with electrodynamics, the persistent current in the Josephson junction ring is given by

$$I = \frac{d\langle E_J \rangle}{d\Phi} = \frac{1}{\Phi_0} \frac{d\langle E_J \rangle}{d\phi}, \quad (11)$$

where averaging is performed over quantum fluctuations with the help of the statistical model of Eq. (9). At $U = 0$, when quantum fluctuations are absent, substitution into this formula of the ground-state energy $E_J^{(0)}(\Phi)$ given by Eq. (4) results at large N in $I(\Phi)$ shown in Fig. 2b. For, e.g., half a fluxon, $\Phi = \Phi_0/2$, the current has the same absolute value but flows in opposite directions for $m = 0$ and $m = -1$. Any non-zero U permits quantum tunneling between such current states that has been observed in experiment^{21,22}. Eq. (3) yields

$$\begin{aligned} \langle E_J \rangle &= NJ \left[1 - \left\langle \cos \left(\tilde{\theta}_{i+1,l} - \tilde{\theta}_{i,l} + \frac{2\pi(\phi + m_l)}{N} \right) \right\rangle \right] \\ &= NJ \left[1 - \left\langle \cos \frac{2\pi(\phi + m_l)}{N} \cos(\tilde{\theta}_{i+1,l} - \tilde{\theta}_{i,l}) \right\rangle \right. \\ &\quad \left. + \left\langle \sin \frac{2\pi(\phi + m_l)}{N} \sin(\tilde{\theta}_{i+1,l} - \tilde{\theta}_{i,l}) \right\rangle \right]. \quad (12) \end{aligned}$$

Note that quantum fluctuations involve both, fluctuations of the reduced phases $\theta_{i,l}$ and the phase slips corresponding to the transitions between different m -numbers. The latter leads to different values of $m = m_l$ at different moments of the discrete imaginary time l .

At small U satisfying $T^* = \sqrt{2JU} \ll T_c \sim J$ the phase slips have exponentially small probability. Consequently, at a small T^* , if one induces a persistent current by placing the Josephson junction ring in the magnetic field, the phase slips may not occur on the time scale of the experiment. In this case the energy simplifies to

$$\langle E_J \rangle = NJ \left[1 - \cos \frac{2\pi(\phi + m)}{N} \left\langle \cos(\tilde{\theta}_{i+1,l} - \tilde{\theta}_{i,l}) \right\rangle \right], \quad (13)$$

since $\left\langle \sin(\tilde{\theta}_{i+1,l} - \tilde{\theta}_{i,l}) \right\rangle = 0$. The persistent current computed with the help of Eqs. (11) becomes

$$I = \frac{2\pi J}{\Phi_0} \sin \left(\frac{2\pi(\phi + m)}{N} \right) \langle \cos(\tilde{\theta}_{i,l} - \tilde{\theta}_{i+1,l}) \rangle. \quad (14)$$

This expression corresponds to the spin-wave approximation in which the effect of the magnetic flux and the global phase change m have been factored out.

We now recall that the statistical mechanics of our model is that of the $2d$ xy model at $T = T^*$, for which the low-temperature (spin-wave) result is¹⁹:

$$\langle \cos(\theta_i - \theta_{i+\delta}) \rangle = 1 - \frac{T^*}{4J}, \quad (15)$$

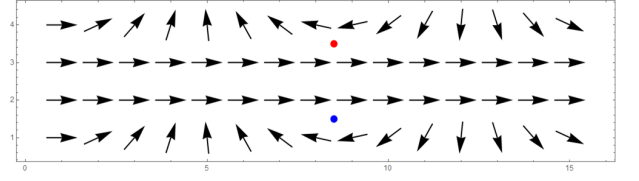


Figure 4: Phase slip in $2d$ xy model via creation of the vortex-antivortex pair.

δ being the nearest neighbor in any direction. This gives

$$\begin{aligned} I &= \frac{2\pi J}{\Phi_0} \sin \left(\frac{2\pi(\phi + m)}{N} \right) \left(1 - \frac{T^*}{4J} \right) \\ &\cong \frac{(2\pi)^2 J}{N\Phi_0} (\phi + m) \left[1 - \left(\frac{U}{8J} \right)^{1/2} \right] \quad (16) \end{aligned}$$

for the persistent current in the "spin-wave" limit. In the last equation we have used $\sin[2\pi(\phi + m)/N] \cong 2\pi(\phi + m)/N$ at large N . As we shall see, this formula agrees well with numerical results.

Phase slips require creation of vortex-antivortex pairs, as is illustrated schematically in Fig. 4. The phase of each superconducting island is represented by the spin vector $\mathbf{s}_r = (\cos\theta_r, \sin\theta_r)$. The vortex (blue dot) is shown at the center of the plaquette for which, on the way counterclockwise, the spin is rotating by 2π . For the antivortex (red dot) the spin is rotating by -2π . Horizontal direction represents the $1d$ ring, while the vertical direction represents the imaginary time. In the two central rows $m = 0$ while in the top and bottom rows $m = 1$. In the absence of the magnetic flux, the current in the two central rows is zero. To the contrast, in the top and the bottom rows there is a current due to the phase gradient. Slow spatial rotation of the spins in these rows eventually makes them strongly non-collinear with the spins in the central rows, which, inevitably, leads to the creation of singularities – vortices and antivortices. A closely-bound vortex pair has the energy of order J , thus at $T^* \ll J$ the concentration of vortex pairs is exponentially small. This is why the phase slips can be ignored in the spin-wave approximation. If the distance between the vortex and the antivortex in the pair increases, the area where the current is disturbed also increases. However, an additional energy, that is logarithmic on the separation, is required to break the pair. According to the established scenario, the vortex pairs unbind at the temperature $T^* = T_{KT}$ of the Kosterlitz-Thouless transition. This would mean unlimited proliferation of the phase slips and the complete destruction of the persistent current.

In the half-fluxon case, even below the Kosterlitz-Thouless transition, vortices provide phase slips that make the persistent current to tunnel between opposite directions. If one allows sufficient real or computer time, it makes the initially created persistent current to evolve to the zero average corresponding to a superposition of clockwise and counterclockwise currents. It is instructive to compare the Josephson ring with the Ising system

of a finite size. In the thermodynamic limit, $N \rightarrow \infty$, the $2d$ and $3d$ Ising models possess the order parameter – magnetization. This happens, because the transition from the state with the magnetization looking up to the state with the magnetization looking down requires the formation of the domain wall that traverses the system. Its energy scales as the size of the system N . To the contrast, the persistent current is a mesoscopic quantity, $I \propto 1/N$, that disappears in the thermodynamic limit. If, instead, one deals with the quantity NI , the dependence of the phase-slip barrier on N becomes important. Since only one vortex-antivortex pair is needed for the phase slip, the corresponding barrier can only have logarithmic dependence on N . Consequently, one should expect that increasing the system size will not stabilize the persistent current. Thus, the latter cannot play the role of the order parameter similar to the magnetization in the Ising model. A more detailed analysis of the barrier associated with the phase slip will be presented in Section IV.

III. NUMERICAL RESULTS

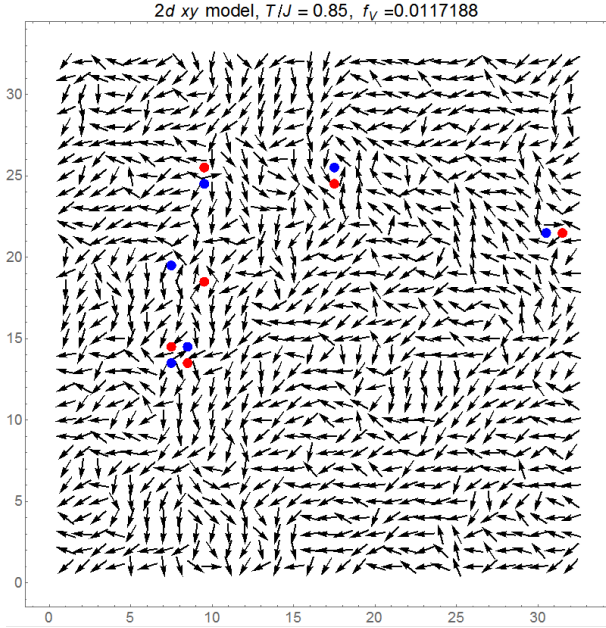


Figure 5: Color online: Vortex pairs in the $2d$ xy model providing phase slips in the quantum Josephson-junction ring.

A. Numerical method

To solve the problem numerically, it is convenient to rewrite the effective classical Hamiltonian \mathcal{H}_{1+1} of Eq. (10) in terms of the classical spin vectors $\mathbf{s}_{\mathbf{r}} =$

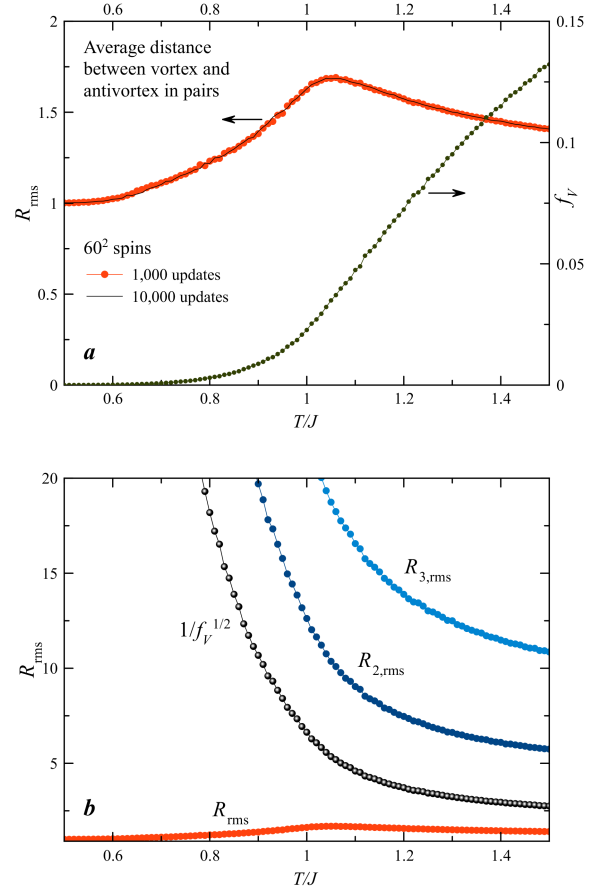


Figure 6: Color online: Vorticity f_V and the average distance between vortices and antivortices in pairs vs T . (a) Vorticity and distance in the pairs; (b) Distances between the nearest (R_{rms}), next-nearest ($R_{2,\text{rms}}$), and next-next-nearest ($R_{3,\text{rms}}$) neighbors of a vortex, as well as the average distance between singularities $1/\sqrt{f_V}$.

$$(\cos \theta_{\mathbf{r}}, \sin \theta_{\mathbf{r}}),$$

$$\mathcal{H}_{1+1} = -\frac{1}{2} \sum_{\mathbf{r}\mathbf{r}'} J_{\mathbf{r}\mathbf{r}'} \mathbf{s}_{\mathbf{r}} \cdot \mathbb{R}_{\mathbf{r}\mathbf{r}'} \cdot \mathbf{s}_{\mathbf{r}'}, \quad (17)$$

where

$$\mathbb{R}_{\mathbf{r}\mathbf{r}'} = \begin{pmatrix} \cos \phi_{\mathbf{r}\mathbf{r}'} & -\sin \phi_{\mathbf{r}\mathbf{r}'} \\ \sin \phi_{\mathbf{r}\mathbf{r}'} & \cos \phi_{\mathbf{r}\mathbf{r}'} \end{pmatrix} \quad (18)$$

and $\phi_{\mathbf{r}\mathbf{r}'}$ are defined below Eq. (10).

Averages of physical quantities at temperature T^* are computed by a combination of standard Metropolis updates and over-relaxation. In a Metropolis update, a spin is rotated by a random trial angle and the corresponding energy change ΔE is computed. If $\Delta E < 0$, the rotation is accepted. If $\Delta E > 0$, the rotation is accepted with probability $\exp(-\Delta E/T^*)$. To keep the acceptance rate not too small and not too large, the trial angles are kept within the interval that increases with T^* . The so-called over-relaxation flips the spin over the

effective field $\mathbf{H}_{\text{eff},\mathbf{r}} = -\partial\mathcal{H}_{1+1}/\partial\mathbf{s}_{\mathbf{r}}$ according to $\mathbf{s}_{\mathbf{r}} \Rightarrow 2(\mathbf{s}_{\mathbf{r}} \cdot \mathbf{h}_{\text{eff},\mathbf{r}})\mathbf{s}_{\mathbf{r}} - \mathbf{s}_{\mathbf{r}}$, where $\mathbf{h}_{\text{eff},\mathbf{r}} = \mathbf{H}_{\text{eff},\mathbf{r}}/H_{\text{eff},\mathbf{r}}$. Over-relaxation is, in fact, a kind of a conservative pseudo-dynamics. For each spin, Metropolis update was done with the probability α and the over-relaxation was done with the probability $1 - \alpha$. The constant α plays the role of the damping in our computations. This routine is performed on all spins sequentially. Updating all spins means one complete update. It is well-known that for classical spin systems mixing over-relaxation with the Monte Carlo routine increases the performance of the numerical method. Metropolis updates cause dynamics of a diffusive type, making the system to explore its phase space slowly. Over-relaxation is a fast ballistic process covering the phase space fast. In our problem, pure Monte Carlo ($\alpha = 1$) does not result in switching of the current in the half-fluxon case via transitions that require creation and unbinding of the vortex-antivortex pairs. Thus, using pure Monte Carlo one can erroneously conclude that the current is stable. However, when the over-relaxation is dominant ($\alpha \ll 1$) the current is switching directions at the elevated temperatures.

Most of the numerical results were obtained with a two-stage process. First, 300 updates with $\alpha = 1$ were done to equilibrate the system at a certain temperature. Then, a large number (up to 10^5) of updates with $\alpha = 0.01$ were done for each temperature to explore the phase space and to allow the switching of the current. The temperature was typically increased or decreased in small steps ($\Delta T^*/J = 0.01$) that provided an additional possibility for equilibration. Finally, similar runs of the above routine were conducted in parallel on a multi-core computer and averaging over the runs was performed.

In numerical work we use the original phases of Eq. (1), represented by spin vectors. They are more convenient than the reduced phases $\tilde{\theta}_i$ since both phases and quantum numbers m are fluctuating at elevated temperatures. The average m was computed as

$$\langle m \rangle = \frac{1}{2\pi} \left\langle \sum_i (\theta_{i+1} - \theta_i) \right\rangle, \quad (19)$$

c.f. Eq. (2) that is exponentially close to an integer at low temperatures.

The software used was Wolfram Mathematica that allows compilation (including usage of an external C compiler that doubles the speed) and parallelization. The main operating computer was Dell Precision T7610 Workstation with two Intel Xeon Processors E5-2680 v2 (10 Core, 2.8GHz each). Mathematica could use 16 cores out of 20. The largest-scale computations were done for size 256^2 ($N = 256$) with 100,000 updates, size 512^2 with 10,000 updates, and size 1000^2 with 3,000 updates for each temperature. The number of runs was about hundred (see indicated in figures).

B. Vortex pairs in the effective classical $2d$ xy model

The underlying classical $2d$ xy model has been intensively studied in the past, making the Kosterlitz-Thouless transition the likely mechanism of the destruction of the persistent current by quantum fluctuations at the effective quantum temperature $T^* = T_{KT}$. However, in the context of the phase slips that occur in a quantum $1d$ model, the numerical study of the unbinding of vortices is missing and will be presented here.

Fig. 5 shows thermally excited vortex-antivortex pairs in a $2d$ xy system of size 32^2 at $T^*/J = 1$ that is slightly above the transition temperature at $T_{KT}/J = 0.89$. One can see that vortices and antivortices are still close to each other, although there is at least one unpaired vortex and one unpaired antivortex. Fig. 6a shows the vorticity f_V , defined as the number of vortices and antivortices together per plaquette, for the system of size 60^2 . Temperature dependence of the average root-mean-square distance R_{rms} between vortex and antivortex in the pair is shown as well. The vorticity is exponentially small at low temperatures and it reaches the limiting value $1/3$ at $T \rightarrow \infty$. Near the KT transition the vorticity is still small, $f_V \ll 1$. The distance $R_{\text{rms}} = 1$ on the left side of the plot corresponds to the vortex and antivortex in the pair occupying neighboring plaquettes. With temperature increasing, R_{rms} increases too, as expected. Surprisingly, however, it does not become large near the KT transition, in contrast with the popular narrative of the massive production of free vortices due to the unbinding of pairs at T_{KT} . The reason for this must be that f_V increases with temperature, so that the average distance between singularities, $r^* = a/\sqrt{f_V}$, is decreasing, pressing R_{rms} down. This is illustrated in Fig. 6b showing R_{rms} together with the average distances to the first, second, and third nearest antivortex neighbors for a vortex in a system of size 60^2 . Increasing the system size does not change these results.

C. Destruction of the persistent current by quantum fluctuations

Temperature dependence of the persistent current I in the quarter-fluxon case, $\phi = 1/4$, obtained by decreasing T^* , is shown in Fig. 7 for different system sizes N . In fact, IN is plotted. In such representation the curves for different sizes coincide everywhere except in the region of the KT transition. The spin-wave theory, Eq. (16), works well in the low-temperature region. The curves for different sizes diverge at the temperature very close to $T_{KT} = 0.89J$, becoming steeper with increasing the size. One can project that in the limit $N \rightarrow \infty$ there will be a jump at $T^* = T_{KT}$. However, in this limit the persistent current itself disappears. Since I becomes small for large sizes, its fluctuations grow and one has to perform many runs of computations to average them out. Most of

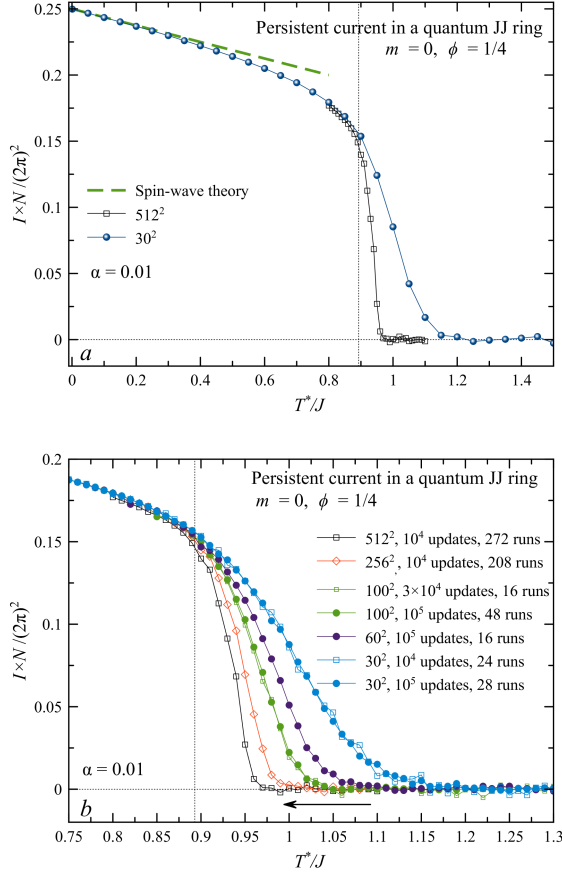


Figure 7: Color online: Dependence of the persistent current on the quantum temperature $T^* = \sqrt{JU}$ for different lattice sizes in the quarter-fluxon case. (a) The entire temperature range. The result of the spin-wave theory is given by Eq. (16). (b) Vicinity of the Kosterlitz-Thouless transition.

the data have been obtained with 10^4 and 10^5 updates, and the results for different numbers of updates coincide. This means that in our computations the system is at equilibrium at any temperature.

Results of computations for the system of size 1000^2 in the half-fluxon case, performed with the intermediate damping $\alpha = 0.1$ and a moderate number 3000 of updates for each temperature increased in small steps (without pre-thermalization with $\alpha = 1$), are shown in Fig. 8. At the first sight $I(T^*)$ looks like the temperature dependence of the order parameter that for the biggest system size disappears at $T^*/J \approx 0.97$. The numerical data at low temperatures are very smooth and precise, while the agreement with the spin-wave theory, Eq. (16), is excellent. However, there are considerable fluctuations in a wide critical region, even for a large system size. They are related to the smallness of the current, $I \propto 1/N$. The average phase change $\langle m \rangle$ of Eq. (19) is exponentially close to an integer set as the initial condition at low temperatures. This justifies the approximation made in the derivation of Eq. (16). Temperature dependence of $\langle m \rangle$

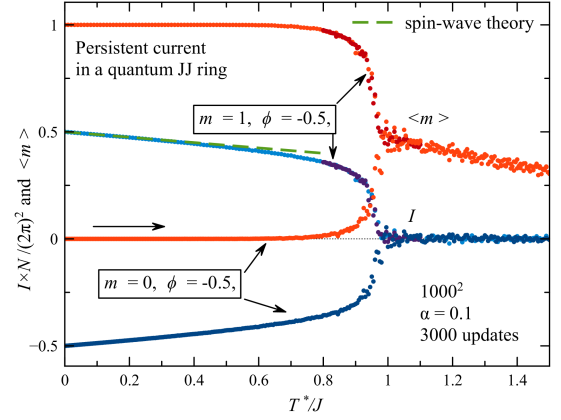


Figure 8: Color online: Dependence of the persistent current and the average phase change $\langle m \rangle$ on increasing T^* in the half-fluxon case for the intermediate damping ($\alpha = 0.1$) and a moderate number of updates. Green dashed line is the spin-wave result of Eq. (16).

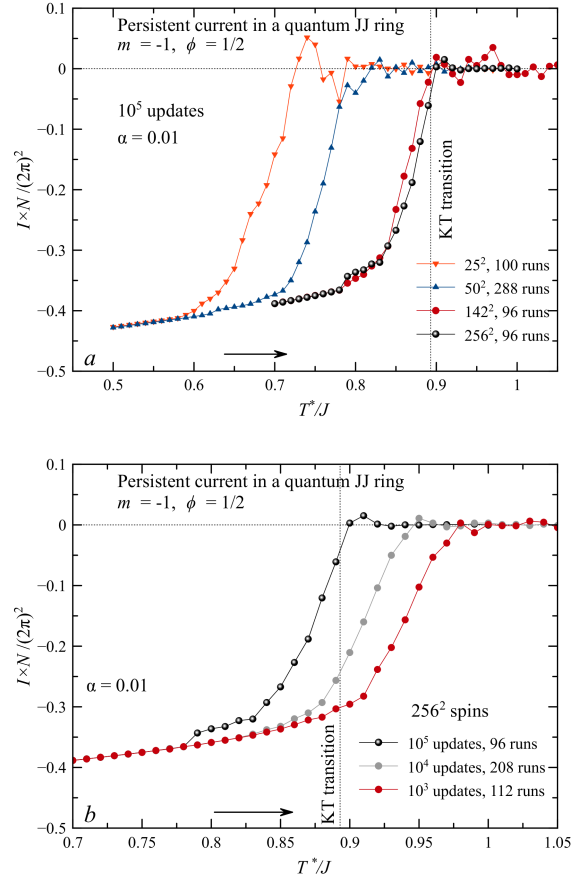


Figure 9: Color online: Dependence of the persistent current on T^* in the half-fluxon case. (a) For different sizes with low damping ($\alpha = 0.01$) and large number of updates; (b) For different numbers of updates.

is due to the creation and unbinding of vortex-antivortex pairs, as explained above.

Computations performed with low damping $\alpha = 0.01$ (making pre-thermalization with $\alpha = 1$) and large number of updates (up to 10^5) show instability of the persistent current in the half-fluxon case, related to its tunneling between the two equal-energy classical states. In Fig. 9a one can see that for small system sizes I is getting destroyed by the jumping to the same-energy state well below the Kosterlitz-Thouless transition temperature. With increasing the size, the curves $I(T^*)$ are shifting to the right and saturate at size 142^2 . This behavior will be explained qualitatively in the next section. Incidentally, for this size and also for $N = 256^2$ the current is disappearing exactly at T_{KT} . This has to be taken with a grain of salt, however. The curves for size 256^2 in Fig. 9b, obtained with temperature increasing, are shifting to the left when more computer time is allowed for relaxation, that is, with the number of updates. Although it would take impractically long computer time to increase the number of updates past 10^5 , one can project that for a sufficient number of updates the persistent current will disappear at any temperature.

IV. ANALYSIS

Here we estimate the energy barrier for the quantum phase slip associated with the unbinding of vortex-antivortex pairs in a system of finite size. The energy of a vortex pair has the form

$$E(r) = 2E_c + 2\pi\rho(T)J \ln(r/a), \quad (20)$$

where $E_c \sim J$ is the vortex core energy, a is the lattice spacing, r is the distance between the singularities in the pair, and $\rho(T)$ is helicity that describes the softening of the system with increasing temperature, $\rho(0) = 1$. Since the energy of the pair increases with the distance, the unbinding takes place in one of two cases: 1) r reaches the linear size of the system $L = a\sqrt{N}$; 2) r reaches $r^* = a/\sqrt{f_V}$, the average distance between singularities. In the latter case realized for $r^* \lesssim L$, vortices and antivortices, after reaching this distance, recombine with the members of other pairs, which facilitates the phase slips. The vorticity and r^* can be estimated as

$$f_V = e^{-2E_c/T}, \quad r^* = ae^{E_c/T}. \quad (21)$$

For $r^* \lesssim L$ the barrier ΔE for the unbinding is given by $E(r^*)$,

$$\Delta E = E(r^*) = 2E_c + \frac{2\pi\rho(T)JE_c}{T}, \quad (22)$$

where the second term is dominant at lower temperatures. One can see that ΔE is independent of the system size. In this case the rate of the vortex-pair unbinding

and, thus, the probability of the phase slip, are proportional to

$$\exp\left(-\frac{\Delta E}{T}\right) \cong \exp\left(-\frac{2\pi\rho(T)JE_c}{T^2}\right), \quad (23)$$

that vanishes quickly at low temperatures. This explains why it is so difficult to obtain numerically the equilibrium result $I = 0$ in the half-fluxon case.

For systems of smaller size at low temperatures there are too few vortices, so that $r^* > L$ and the barrier is given by

$$\Delta E = 2E_c + 2\pi\rho(T)J \ln(L/a). \quad (24)$$

With the second term dominant, this leads to the phase slip (unbinding) rate proportional to

$$\exp\left(-\frac{\Delta E}{T}\right) \cong \left(\frac{a}{L}\right)^{2\pi\rho(T)J/T} = \frac{1}{N^{\pi\rho(T)J/T}}, \quad (25)$$

which decreases with the system size. One can see in Fig. 9a that for small sizes $I(T^*)$ is shifting to the right in accordance with Eq. (25) and then saturates in accordance with Eq. (23).

V. DISCUSSION

We have studied the dependence of the persistent current in a Josephson junction ring on the strength of quantum fluctuations, U/J , the number of superconducting islands, N , and the flux threading the ring, $\phi = \Phi/\Phi_0$. All three parameters can be controlled in experiment. The strength of quantum fluctuations is determined by the Josephson coupling of the islands and their capacitances. At some critical U/J the system undergoes a quantum phase transition into the superinsulator state characterized by zero conductivity of the ring in the presence of the superconductivity of the islands. Persistent current presents a good experimental tool for the investigation of this transition.

From theoretical perspective the problem allows accurate numerical studies by Monte Carlo techniques developed for spin systems because it maps onto a classical $2d$ xy model at finite temperature. In this approach the critical strength of quantum fluctuations projects onto the temperature of the Kosterlitz-Thouless phase transition. The numerical solution of the problem is, however, significantly more challenging than equilibrium problems of spin physics because the persistent current disappears in the thermodynamic limit $N \rightarrow \infty$.

In accordance with the expectation we find that in all cases the persistent current is destroyed by sufficiently strong quantum fluctuations. The manner in which it is destroyed depends strongly on the number of superconducting islands in the Josephson junction ring and on the magnetic flux threading the ring. In cases of a half-integer flux, $\phi = n + 1/2$, when the classical ground state

of the ring is degenerate, quantum fluctuations of any strength in theory destroy the persistent current. However, the phase slips required for that have a finite probability that is exponentially small at $U \ll J$. In that sense, the persistent current in the presence of weak quantum fluctuations is as stable as the magnetic moment of a superparamagnetic particle below the blocking temperature. Unlike the magnetization of a superparamagnetic particle (or of a finite-size Ising system) though, the persistent current cannot be made stable by increasing the system size. This is because the barrier for the switching of the current due to the quantum phase slip becomes size independent for large sizes. For small Josephson rings, we find that quantum fluctuations destroy the persistent current even faster. However, the dependence on the size is at best logarithmic. This finding can be of interest to the experimentalists.

When the classical ground state is not degenerate, the persistent current has a non-zero equilibrium value. At $U \ll J$ the spin-wave approximation provides an excellent agreement with the numerical data on how the per-

sistent current decreases when the strength of quantum fluctuations increases. The behavior is independent of the size of the ring. This prediction of the theory would be interesting to test in a real experiment. Another interesting prediction is that the departure from the universal behavior towards the behavior that depends on the size of the ring begins at the critical strength of quantum fluctuations determined by the bulk Kosterlitz-Thouless temperature. We present numerical study of the phase slips due to the unbinding of vortex-antivortex pairs and analytical arguments that explain the size-dependence of the persistent current.

VI. ACKNOWLEDGEMENTS

This work has been supported by the grant No. DE-FG02-93ER45487 funded by the U.S. Department of Energy, Office of Science.

-
- ¹ See, e.g., S. L. Sondhi, S. M. Girvin, J. P. Carini, and D. Shahar, Continuous quantum phase transitions, *Review of Modern Physics* **69**, 315-333 (1997).
 - ² S. Sachdev, *Quantum Phase Transitions* (Cambridge University Press, Cambridge, UK, 2011).
 - ³ L. B. Ioffe, M. V. Feigel'man, A. Ioselevich, D. Ivanov, M. Troyer, and G. Blatter, Topologically protected quantum bits using Josephson junction arrays, *Nature* **415**, 503-506 (2002).
 - ⁴ S. Gladchenko, D. Olaya, E. Dupont-Ferrier, B. Doucot, L. B. Ioffe, and M. E. Gershenson, Superconducting Nanocircuits for Topologically Protected Qubits, *Nature Physics* **5**, 48-53 (2009).
 - ⁵ V. E. Manucharyan, J. Koch, L. I. Glazman, and M. H. Devoret, Fluxonium: Single Cooper-Pair Circuit Free of Charge Offsets, *Science* **326**, 113-116 (2009).
 - ⁶ A. D. Zaikin, D. S. Golubev, A. van Otterlo, and G. T. Zimanyi, Quantum phase slips and transport in ultrathin superconducting wires, *Physical Review Letters* **78**, 1552-1555 (1997).
 - ⁷ D. S. Golubev and A. D. Zaikin, Quantum tunneling of the order parameter in superconducting nanowires, *Physical Review B* **64**, 014504-(14) (2001).
 - ⁸ G. Rastelli, I. M. Pop, and F. W. J. Hekking, Quantum phase-slips in Josephson junction rings, *Physical Review B* **87**, 174513-(18) (2013).
 - ⁹ R. M. Bradley and S. Doniach, Quantum fluctuations in chains of Josephson junctions, *Physical Review B* **30**, 1138-1147 (1984).
 - ¹⁰ S. E. Korshunov, Effect of dissipation on the low-temperature properties of a tunnel-junction chain, *Soviet Physics JETP* **68**, 609-618 (1989).
 - ¹¹ E. Chow, P. Delsing, and D. B. Haviland, Length-scale dependence of the superconductor-to-insulator quantum phase transition in one dimension. *Physical Review Letters* **81**, 204-207 (1998).
 - ¹² See review and references therein: J. E. Mooij, G. Schön, A. Shnirman, T. Fuse, C. J. P. M. Harmans, H. Rotzinger, and A. H. Verbruggen, Superconductor-insulator transition in nanowires and nanowire arrays, *New Journal of Physics* **17**, 033006-(12) (2015).
 - ¹³ See, e.g., G. Schwiete and Y. Oreg, Persistent current in small superconducting rings, *Physical Review Letters* **103**, 037001-(4) (2009), and references therein.
 - ¹⁴ M. Y. Choi, Persistent current and voltage in a ring of Josephson junctions, *Physical Review B* **48**, 15920-15925 (1993).
 - ¹⁵ K. A. Matveev, A. I. Larkin, and L. I. Glazman, Persistent current in superconducting nanorings, *Physical Review Letters* **89**, 096802-(4) (2002).
 - ¹⁶ M. Lee, M.-S. Choi, and M. Y. Choi, Quantum phase transitions and persistent currents in Josephson-junction ladders, *Physical Review B* **68**, 144506-(11) (2003).
 - ¹⁷ I. M. Pop, I. Protopopov, F. Lecocq, Z. Peng, B. Pannetier, O. Buisson, and W. Guichard, Measurement of the effect of quantum phase-slips in a Josephson junction chain, *Nature Physics* **6**, 589-592 (2010).
 - ¹⁸ M. Tinkham, *Introduction to Superconductivity* (Dover Publications, 2004, ISBN 0-486-43503-2).
 - ¹⁹ J. Tobochnik and G. V. Chester, Monte Carlo study of the planar spin model, *Physical Review B* **20**, 3761-3769 (1979).
 - ²⁰ R. Gupta and C. F. Baillie, Critical behavior of the two-dimensional XY model, *Physical Review B* **45**, 2883-2898 (1992).
 - ²¹ J. R. Friedman, V. Patel, W. Chen, S. K. Tolpygo, and J. E. Lukens, Quantum superposition of distinct macroscopic states, *Nature* **406**, 43-45 (2000).
 - ²² C. H. van der Val, A. C. ter Haar, F. K. Wilhelm, R. N. Schouten, C. J. Harmans, T. P. Orlando, S. Lloyd, and J. E. Mooij, Quantum superposition of macroscopic persistent-current states, *Science* **290**, 773-777 (2000).